Second-order Raman spectroscopy of char during gasification

Shuai Wang, Tingting Li, Liping Wu, Lei Zhang, Li Dong, Xun Hu and Chun-Zhu Li*

Fuels and Energy Technology Institute, Curtin University of Technology, GPO Box U1987, Perth, WA 6845, Australia

Submitted to

Fuel Processing Technology

For consideration for publication in

the Special Issue: 2014 Australia-China Symposium on Energy

July 2014

*Corresponding author: chun-zhu.li@curtin.edu.au; telephone: +61 8 9266 1131; facsimile: +61 8 9266 1138

Abstract

Raman spectroscopy has been widely used in the structural characterisation of various carbonaceous materials. Through spectral deconvolution, FT-Raman spectroscopy has been used to gain insights into the transformation of char structure during gasification, providing new evidence to understand the char gasification mechanisms. These studies have mainly focused on the first-order Raman spectra in the range between 800 and 1800 cm^{-1}. Additional information can be gained from the second-order Raman spectra. This study aims to develop a new spectral deconvolution scheme for the second-order Raman spectra of chars from the gasification of coal and biomass. As our initial attempt, the second-order Raman spectra of chars in the range between 2,000 and 3,300 cm^{-1} were deconvoluted into 7 bands representing the main structural features in the chars. Both total Raman peak area and band area ratios are used to gain information about the structural features of char. Using chars from the gasification of WA Collie sub-bituminous coal in CO_2 and H_2O as examples, the implication of the first-order and second-order Raman spectral data in terms of gasification mechanisms is discussed.

Keywords: Raman spectroscopy; Second order; Char structure; Gasification; Coal; Biomass

1. Introduction

Gasification is an effective method to convert a solid fuel into a high value gaseous fuel [1]. An important aspect of gasification is the reaction between char and gasifying agents to produce syngas [2]. This is a heterogeneous gas-solid reaction and is very complicated as a result of changes in the char structure during gasification [2,3]. Therefore, understanding the transformation of structural feature of char during gasification and the effects of char structure on its gasification reactivity is critically important for a better understanding of the gasification mechanisms [4-7].

Raman spectroscopy has been widely used as a powerful tool to characterise various carbonaceous materials due to its ability to response to symmetric vibration of less or non-polar bonds [8,9]. A Raman spectrum represents the scattering due to many types of distinctly different bonds in the char. There are two Raman spectral regions, in the ranges of ~ 800 to 1800 cm^{-1} (first order) and ~ 2,000 to 3,300 cm^{-1} (second order), that are of interests in understanding the structural features of a carbonaceous material. Much has been done to investigate the char structure through deconvolution and analysis of various bands in the first-order Raman spectra [10-15]. Like a first-order Raman spectrum, a second-order Raman spectrum is also the summation of scattering from many bonds. If deconvoluted properly, a second-order spectrum can also provide additional detailed information about the skeletal structure of a carbon-based material. However, second-order Raman spectroscopy has been mainly used for the characterisation of highly ordered carbon materials such as graphite [9,16,17]. Little study has been carried out on the highly disordered carbon materials such as chars from the pyrolysis and gasification of coal and biomass. Even for some research that analysed the second-order Raman

spectrum of some highly disordered carbon materials [18-25], most samples have undergone a high temperature treatment (higher than 1000 ˚C) [18,19,24,25], resulting in the samples have become crystallisation and graphitization. Therefore, the second-order Raman spectra of such samples were simply deconvoluted into three or four bands and the interpretation of these bands follow the bands assignment of highly ordered carbon materials [19-25].

Obviously, the second-order spectra of chars from the pyrolysis and gasification process (<1000 ˚C) differ considerably from that of highly ordered materials or highly graphitized materials. A simple adoption of the concept of bands in the second-order spectra for highly ordered carbon materials would be very inappropriate for the analysis of char structure. Unlike the second-order spectra of graphite-like materials that exhibit a clearly-resolved strong peak of 2D (overtone of D band) and a peak of D+G (combination of D band and G band) [9,16,17], the second-order spectrum of a char could show a very broad band. The overlaps between the 2D and D+G bands as well as the shoulders at the two sides of the 2D and D+G broad bands in the second-order Raman spectrum of a char could contain much information about the structural feature of the char. Therefore, instead of just considering the 2D and G+D bands, the second-order Raman spectrum could be deconvoluted into more bands in order to acquire detailed information about the chemical structure of the char. In addition, because of the differences in crystal structure between graphite and amorphous carbon, simple applications of the interpretation of the second-order Raman spectra of highly ordered materials to chars would result in some misleading information and miss some important information about the skeletal carbon structures.

In our previous study [26], a WA Collie sub-bituminous coal was gasified at different temperatures (800, 850 and 900 ˚C) in atmospheres containing steam and CO_2. The Raman spectra of char samples collected after varying extents of gasification were acquired by using a laser with a wavelength of 1,064 nm [11,26]. In this study, the same spectra in the second-order region have been analysed. Compared with our previous work [4,6,7,11-15,26] which mainly focused on the analysis of the first-order Raman spectra, a new spectral deconvolution method for the Raman spectra in the second-order region was established in order to acquire detailed information about the changes in char structure during gasification. The information about char structure from the second-order region is compared with that of the first-order region and complementary or additional information was found through analysis of the second-order Raman spectra.

2. Experimental

2.1 Gasification of coal

The details of the gasification experiments have been presented previously [26]. Briefly, Collie sub-bituminous coal, supplied by the Muja Power Station in Western Australia, was used. It has an ultimate composition of 75.7% C, 4.5% H, 1.4% N, 0.5% S and 17.9% O [26]. The gasification experiments were carried out in a fluidised-bed/fixed-bed reactor [26,27] with coal particles being heated up rapidly.

2.2 Char characterisation

The acquisition of Raman spectra of chars were detailed before [26]. The same spectra were used in this study. Briefly, a Perkin-Elmer Spectrum GX FT-IR/Raman spectrometer with an excitation laser of 1,064 nm was used to acquire the Raman spectra of chars [11,26]. A char sample was firstly ground into powder and then diluted and ground with spectroscopic grade KBr [11,26]. The char concentration of 0.25 wt% in KBr-char mixture exhibited the plateau total Raman intensity in the first-order Raman region [26]. The total Raman peak area in the second-order Raman region had also reached the plateau with this char concentration as shown in Figure 1. An InGaAs detector was used to collect Raman scattering using a back scattering configuration [11,26]. Each spectrum represents the average of 200 scans and the spectral resolution was 4 cm^{-1} [11,26]. Baseline correction was carried out on each spectrum using the software provided by Perkin-Elmer with the spectrometer [11,26]. The first-order and second-order regions had different baselines.

3. Deconvolution and band assignment of the second-order Raman spectra

The second-order Raman spectra of chars in the range between 2,000 and 3,300 cm^{-1} were curve-fitted with 7 mixed Gaussian and Lorentz bands using the GRAM/32 software. The position and assignment of these 7 bands are briefly summarized in Table 1, which we believe represent the typical structural features of chars from the pyrolysis and gasification of coal and biomass.

In the second-order spectra of sp^2 carbon materials, there is a strong Raman feature appearing in the range of 2,500-2,700 cm^{-1}, and it is called the 2D band to mean that it is the overtone of D band in the first-order region [9,16,17]. In the study

of the second-order Raman spectra of highly ordered carbonaceous materials, the 2D band was considered to originate from a double resonance, involving two iTO phonons near the *K* point of the unit cell [9]. The intensity of the 2D band was believed to be related to the number of grapheme layers and the stacking order [9,16,17]. Unlike the defect-induced D band in the first-order region, the 2D band does not indicate any kinds of disorder or defect for the graphite-like material [9,16,17,28,29]. However, the “crystal” structure of char is quite different from the graphite-like carbon materials. Chars from the pyrolysis and gasification of coal and biomass are highly disordered carbonaceous materials with a wide variety of O-containing groups and sp^2-sp^3 or sp^3-sp^3 cross-linking structures [11]. According to the bands assignment for the highly dis-ordered materials [11], the D band mainly represents aromatics with not less than 6 rings. For graphitic materials, the D band and 2D band come from two different physical scattering processes so there is no direct relationship in band intensity between these two bands [9,16,17,28,29]. However, a char from the gasification of coal or biomass does not have similar lattice structure and therefore its D and 2D bands do not necessarily originate from two scattering processes. Based on the vibrational theory of the overtone process for chemical structures [8,30], it is believed that the D band and the 2D band come from the same vibration mode for the amorphous carbon materials. Therefore, the interpretation of the 2D band in the second-order spectra of char should be the same as the D band in the first-order [11], i.e. representing the large aromatic ring systems (no less than 6 fused rings). It is also expected to have close relationship with the D band in term of the band intensity in the second-order Raman spectra.

Another main band in the second-order spectra of carbonaceous materials is the D+G band located in the range of 2800-2950 cm^{-1} with an exciting laser in the visible

range [16,17,24,25]. In the study of the highly ordered carbon materials, this band is considered as a disorder-induced band and would disappear with increasing crystallinity [16,24]. Amorphous carbon materials such as char from gasification would not have a band of the same nature in their second-order spectra. Instead, in this study, the D+G band is assigned to the aromatic ring structures of amorphous carbon materials.

Different from the graphite-like materials, vast amounts of spectral residue would be left if only 2D and D+G bands were considered to deconvolute the second-order Raman spectra of chars. Based on the spectra of some model aromatic compounds [30] and considering the structure of char from coal/biomass gasification process [11-15], two bands have been assigned in the region between the 2D band and D+G band. One is the overtone of the fundamental vibrations of aryl methyl functional groups at around 2,750 cm^{-1} [30] and named as $2V_R$ (in order to correspond with the band name V_R in the first-order [11]). The other is the $(2D)_L$ band (standing for 2D left) at around 2,650 cm^{-1}. These two bands are mainly found in amorphous carbon materials [24,25,30]. In this case, $2V_R+(2D)_L$ can represent the small aromatic ring systems, and it is believed to decrease with the condensation of aromatic ring systems according to some Raman spectra of amorphous carbon materials that have been heat-treated at high temperature [24,25].

In addition, there is a weak peak [16,25,31,32] in the range of 2350-2500 cm^{-1} that can be found in the second-order Raman spectra of some highly ordered carbon materials by an exciting laser in the visible range, showing no dispersive behaviour with different laser excitation energy [31,32]. Some believe that this band is related to 2LO phonons second-order scattering [31], while others explain that this band originates from the combination of the D band and the modulation around 1,100 cm^{-1}

[32]. Based on the band assignment in the first-order Raman spectra [11], in the second-order Raman spectra of chars by an exciting laser at 1,064 nm, the frequency of this band is almost twice of that of the S band. Therefore, in this study, this band is assigned to the overtone of S band, named as 2S band, representing the sp^3-rich structures, sp^2-sp^3 carbonaceous structures and other cross-linking structures in char.

In addition to the five bands assigned above, other two bands, a $(D+G)_L$ band (standing for D+G band left) at 3,060 cm^{-1} [28] and a 2G band (overtone of G band) at 3,180 cm^{-1} [16,25], were assigned to the aryl CH vibration and aromatic ring structures respectively.

During spectral deconvolution, band positions were fixed whilst different maximum limits were applied to restrain the bandwidths. A typical example of the spectral deconvolution/curve-fitting of a second-order Raman spectrum of char using the 7 bands is shown in Fig. 2. Similar degrees of successful curve-fitting can be found for all other char samples investigated in this study.

Although the second-order Raman spectra of chars were curve-fitted with 7 bands, the discussion of Raman spectroscopic data will be mainly focused on three bands, 2D, $2V_R+(2D)_L$ and 2S, which represent the main chemical structure in char and are much sensitive to the structural changes. D+G band and two other minor bands, 2G and $(D+G)_L$, actually represent the typical aromatic structures in carbon-based materials and are less sensitive to the structural changes. Thus, they will not be discussed further here.

4. Results and discussion

4.1 Total peak areas of the second-order Raman spectra of chars from the gasification of WA Collie sub-bituminous coal

The observed Raman intensity would be affected by both Raman light scattering ability and the light absorption ability of char. In the first-order region, the electron-rich structures such as the O-containing groups in char tend to have high Raman scattering ability mainly due to the resonance effect between O and O-connected aromatic ring [11]. Therefore, their presence tends to increase the total first-order Raman intensity [11]. On the other hand, the increasing condensation of the aromatic ring systems in char would increase the light absorptivity and thus tends to decrease the observed Raman intensity [11].

The presence of O-containing structures and the condensation of aromatic ring systems are expected to have effects on the observed second-order Raman intensity similar to those in the first order region. Figure 3 exhibits the total peak areas of the second-order Raman spectra in the region of 2000-3300 cm^{-1}, considered as the total second-order Raman intensity, of chars as a function of the gasification holding time. For the chars produced from the gasification in steam-containing atmospheres (15% H_2O-Ar and 15% H_2O-CO_2), the total second-order Raman intensity increased with increasing gasification temperature and holding time. However, the second-order total Raman intensity is almost constant (with large scatters) for the chars produced from the gasification in pure CO_2. These results are consistent with the first-order Raman data [26]. These two different behaviours in terms of the total Raman intensity indicate that the gasification reaction mechanisms of char in H_2O and CO_2 atmospheres are different [26]. The results suggest that the oxygen-

containing species derived from steam increased the O-containing groups in char [26]. With increasing holding time and gasification temperature, more and more O-containing groups have formed, hence increasing the total Raman peak areas of chars obtained from the gasification in steam-containing atmospheres. While for CO_2 gasification, the concentration of such structure is almost constant (with large scatters). In addition, the generally lower total Raman peak areas of chars from gasification in CO_2 indicate that the concentration of O-containing groups in char must be lower for gasification in CO_2 than that in steam.

4.2 Ratios of some major bands to the total Raman intensity in the second-order spectra

4.2.1 The ratio of the 2D band to the total second-order Raman peak area

As are exhibited in Fig. 4, for the chars produced from the gasification in steam-containing atmospheres, a higher temperature resulted in a higher I_{2D}/I_{Total} ratio, indicating the growth in the relative concentrations of large aromatic ring systems in char. In addition, with increasing gasification holding time, the I_{2D}/I_{Total} ratio increased initially before it reached a plateau. The same results can also be found in the first-order Raman in term of the I_D/I_{Total} ratio [26]. However, the change of such intensity ratio is not obvious for the chars from CO_2 gasification in the second-order Raman, possibly because of the low total Raman intensity, and thus the low signal-to-noise ratios for the chars from the gasification in CO_2. Actually, in the first-order Raman, the I_D/I_{Total} ratio increased with increasing gasification temperature and holding time for the chars from CO_2 gasification [26].

4.2.2 The ratio of the $2V_R+(2D)_L$ band to the total Raman intensity

The overlap between the 2D band and the D+G band has been deconvoluted into $2V_R$ band and $(2D)_L$ band, the intensity of these two bands can be taken as a brief reflection of the concentrations of smaller aromatic ring systems in char.

As is shown in Fig. 5, the decreases in the band ratio $I_{2VR+(2D)L}/I_{Total}$ for chars from the gasification in steam-containing atmospheres indicate that the relative concentrations of small aromatic ring systems decreased with increasing gasification temperature and holding time. These results are consistent with the first-order Raman data [26] and suggest that the smaller aromatic ring systems were either preferentially consumed by gasification or converted into large ones during gasification [13-15,26]. On the other hand, for the chars from CO_2 gasification, there is no obvious trend except a possible decrease in the band ratio $I_{2VR+(2D)L}/I_{Total}$ with increasing gasification temperature from 800 to 900 ˚C. However, the relative band ratio $I_{(Gr+Vl+Vr)}/I_{Total}$ in the first-order Raman decreased with increasing gasification temperature and holding time [26]. This difference is also possibly because of the low signal-to-noise ratios in the second-order Raman for the chars from the gasification in CO_2, which made it difficult to resolve weak trends in band area ratios. In addition, the relative concentrations of small aromatic rings in the chars from gasification in CO_2 were higher than those in the chars from gasification in steam-containing atmospheres, also demonstrating that the presence of H radicals from H_2O dissociation can enhance the transition from the relatively small to large aromatic ring systems in char as we revealed in the previous studies [14,15,26].

4.2.4 The ratio of the 2D band to the $2V_R+(2D)_L$ band

The Raman band area ratio $I_{2D}/I_{2VR+(2D)L}$ can be used as a more direct indication of the transition of small to large aromatic ring systems in char samples. As shown in Fig. 6, for the chars produced from the gasification in steam-containing atmospheres, this band area ratio increased with increasing gasification temperature and holding time, which indicate that small aromatics are gradually consumed and/or converted into large ones in char structure. The same trends can also be found in the related ratio $I_D/I_{(Gr+Vl+Vr)}$ in the first-order Raman spectral data [26]. Moreover, the intensity ratio $I_{2D}/I_{2VR+(2D)L}$ of the char from the gasification in pure CO_2 was lower than the char from the gasification in the steam-containing atmospheres. This can also be explained by considering that the H radicals generated by H_2O could penetrate into char matrix and induce the condensation of the aromatic rings [14,15,26], thereby increasing the relative concentrations of large aromatic ring systems in char structure.

4.2.5 The ratio of the 2S band to the total Raman intensity

The intensity of 2S band can be used as indication of the sp^3-rich structures such as alkyl-aryl C-C structures, the crossing-linking density as well as the substitutional groups (other than O-containing ones) in char.

From Fig. 7, it can be seen that, for the gasification in steam-containing atmosphere, the intensity ratio I_{2S}/I_{Total} decreased from 800 to 900 ˚C, and also showed a decrease with increasing holding time and then achieved a plateau value. These results suggested that high temperature and long reaction time tend to cause the loss of the alkyl-aryl C-C structures and the crossing-linking density. There were much less changes in the intensity ratio I_{2S}/I_{Total} if the holding time is long enough, indicating that the amount of such crossing-linking structure in char reached a

dynamic balance between their generation and consumption. For the chars from CO_2 gasification, there is no clear trend for the ratio I_{2S}/I_{Total}, and the data show obvious fluctuations. This is also because that the total Raman intensity of the second-order as well as the 2S band is very weak for the chars from CO_2 gasification, giving rise to high noise-to-signal ratios and causing some inaccuracy during curve-fitting.

An important difference between the first-order and second-order Raman spectra of chars from gasification in steam-containing atmospheres is that the ratio I_S/I_{Total} in the first-order Raman did not change clearly with gasification temperature and holdings time while the ratio I_{2S}/I_{Total} in the second-order Raman showed a decrease with increasing gasification temperature and holding time. It should be noted that there is less interference from the neighbouring bands in the analysis of the intensity of 2S band than that with the S band. Not all peaks in the region of the first-order region have their corresponding peaks in the second-order region, which has facilitated the spectral deconvolution of some bands such as 2S band. Therefore, the second-order Raman spectra can provide additional details about the changes in char structure.

5. Conclusions

This study has demonstrated that the second-order Raman spectroscopy can be used as a powerful technique to analyse the skeletal structure of highly disorder carbon-based materials such as the chars from the gasification of Collie sub-bituminous coal. A novel deconvolution method has been established and the second-order Raman spectra of chars were curved-fitted with 7 bands representing the typical chemical structures in the char.

During the gasification in steam-containing atmospheres, the relative contents of O-containing groups and large aromatic ring systems in char increased, while the relative contents of small aromatic ring systems decreased as gasification proceeded. These results are consistent with the findings in the first-order Raman analysis. However, the second-order spectra of chars from gasification in CO_2 showed high noise-to-signal ratio than the first-order Raman spectra, making the spectral deconvolution of the second-order spectra less reliable than that of the first-order spectra.

Compared with the first-order Raman results, additional information is found in the second-order Raman spectra of chars from the gasification in steam-containing atmospheres. The area ratio I_S/I_{Total} of char did not change clearly with gasification temperature in the first-order Raman spectroscopy. However, there is a significant change with gasification temperature and holding time in the ratio of the overtone of S band (I_{2S}) in the second-order Raman spectroscopy, indicating that the cross-linking density decreased as gasification proceeded.

The second-order Raman spectroscopy of chars from the gasification in CO_2 and H_2O atmospheres indicates that the gasification mechanisms of char in these two atmospheres are different, confirming our earlier conclusions.

Acknowledgements

This study received funding from the Australian Research Council (DP110105514) and the Government of Western Australia. This project was also supported by the Commonwealth of Australia under the Australia-China Science and Research Fund.

References

[1] C-Z Li. Special issue-gasification: A route to clean energy. Process Safety and Environmental Protection 84 (2006) 407-408.

[2] C-Z Li. Importance of volatile-char interactions during the pyrolysis and gasification of low-rank fuels – A review. Fuel 112 (2013) 609-623.

[3] C-Z Li. Some recent advances in the understanding of the pyrolysis and gasification behaviour of Victorian brown coal. Fuel 86 (2007) 1664-1683.

[4] DM Keown, J-I Hayashi, C-Z Li. Drastic changes in biomass char structure and reactivity upon contact with steam. Fuel 87 (2008) 1127-1132.

[5] X Li, H Wu, J-I Hayashi, C-Z Li. Volatilisation and catalytic effects of alkali and alkaline earth metallic species during the pyrolysis and gasification of Victoria brown coal. Part VI. Further investigation into the effects of volatile-char interactions. Fuel 83 (2004) 1273-1279.

[6] X Li, J-I Hayashi, C-Z Li. Volatilisation and catalytic effects of alkali and alkaline earth metallic species during the pyrolysis and gasification of Victoria brown coal. Part VII. Raman spectroscopic study on the changes in char structure during the catalytic gasification in air. Fuel 85 (2004) 1509-1517.

[7] X Li, C-Z Li. Volatilisation and catalytic effects of alkali and alkaline earth metallic species during the pyrolysis and gasification of Victoria brown coal. Part VIII. Catalysis and changes in char structure during gasification in steam. Fuel 85 (2006) 1518-1525.

[8] F Tuinstra, JL Koeing, Raman spectrum of graphite. Journey of Chemical Physics 53 (1970) 1126-1130.

[9] LM Malard, MA Pimenta, G Dresselhaus, MS Dresselhaus. Raman spectroscopy in grapheme. Physics Reports 473 (2009) 51-87.

[10] CA Johnson, JW Patrick, KM Thomas. Characterization of coal chars by Raman spectroscopy, X-ray diffraction and reflectance measurements. Fuel 65 (1986) 1284-1290.

[11] X Li, J-I Hayashi, C-Z Li. FT-Raman spectroscopic study of the evolution of char structure during the pyrolysis of a Victorian brown coal. Fuel 85 (2006) 1700-1707.

[12] H-L Tay, C-Z Li. Changes in char reactivity and structure during the gasification of a Victorian brown coal: Comparison between gasification in O_2 and CO_2. Fuel Processing Technology 91 (2010) 800-804.

[13] H-L Tay, S Kajitani, S Zhang, C-Z Li. Effects of gasifying agent on the evolution of char structure during the gasification of Victoria brown coal. Fuel 103 (2013) 22-28.

[14] DM Keown, X Li, J-I Hayashi, C-Z Li. Evolution of biomass char structure during oxidation in O_2 as revealed with FT-Raman spectroscopy. Fuel Processing Technology 89 (2008) 1429-1435.

[15] X Guo, HL Tay, S Zhang, C-Z Li. Changes in char structure during the gasification of a Victoria brown coal in steam and oxygen at 800 ˚C. Energy Fuels 22 (2008) 4034-4038.

[16] S Vollebregt, R Ishihara, FD Tichelaar, Y Hou, CIM Beenakker. Influence of the growth temperature on the first and second-order Raman band ratios and widths of carbon nanotubes and fibers. Carbon 50 (2012) 3542-3554.

[17] MS Dresselhaus, A Jorio, M Hofmann, G Dresselhaus, R Saito. Perspectives on carbon nanotubes and graphene Raman spectroscopy. Nano Letters 10 (2010) 751-758.

[18] S Dong, P Alvarez, N Paterson, DR Dugwell, R Kandiyoti. Study on the effect of heat treatment and gasification on the carbon structure of coal chars and metallurgical cokes using Fourier Transform Raman Spectroscopy. Energy Fuels 23 (2009) 1651-1661.

[19] A Zaida, E Bar-Ziv, LR Radovic, Y-J Lee. Further development of Raman microprobe spectroscopy for characterization of char reactivity. Proceeding of the Combustion Institute 31 (2007) 1881-1887.

[20] J Jehlicka, C Beny. First and second order Raman spectra of natural highly carbonified organic compounds from metamorphic rocks. Journal of Molecular Structure 480-481 (1999) 541-545.

[21] HJ Seong, AL Boehman. Evaluation of Raman parameters using visible Raman microscopy for soot oxidative reactivity. Energy Fuels 27 (2013) 1613-1624.

[22] A Sadezky, H Muckenhuber, H Grothe, R Niessner, U Poschl. Raman microspectroscopy of soot and related carbonaceous materials: Spectral analysis and structural information. Carbon 43 (2005) 1731-1742.

[23] A Cuesta, P Dhamelincourt, J Laureyns, A Martinez-Alonso, JMD Tascon. Raman microprobe studies on carbon materials. Carbon 32 (1994) 1523-1532.

[24] Y-J Lee. The second order Raman spectroscopy in carbon crystallinity. Journal of Nuclear Materials 325 (2004) 174-179.

[25] S Bernard, O Beyssac, K Benzerara, N Findling, G Tzvetkov, GE Brown. XANES, Raman and XRD study of anthracene-based cokes and saccharose-based chars submitted to high-temperature pyrolysis. Carbon 48 (2010) 2506-2516.

[26] T Li, L Zhang, L Dong, C-Z Li. Effects of gasification atmosphere and temperature on char structural evolution during the gasification of Collie sub-bituminous coal. Fuel 117 (2014) 1190-1195.

[27] DM Quyn, H Wu, J-I Hayashi, C-Z Li. Volatilisation and catalytic effects of alkali and alkaline earth metallic species during the pyrolysis and gasification of Victoria brown coal. Part IV. Catalytic effects of Nacl and ion-exchangeable Na in coal on char reactivity. Fuel 2 (2003) 587-593.

[28] M Ramsteiner, J Wagner. Resonant Raman scattering of hydrogenated amorphous carbon: Evidence for π-bonded carbon clusters. Applied Physics Letters 51 (1987) 1355-1357.

[29] MJ Matthews, MA Pimenta, G Dresselhaus, MS Dresselhaus, M Endo. Origin of dispersive effects of the Raman D band in carbon materials. Physical Review B 59 (1999) 6585-6588.

[30] P Larkin. Infrared and Raman spectroscopy: principles and spectral interpretation. Elsevier: Oxford (2010).

[31] T Shimada, T Sugai, C Fantini, M Souza, LG Cancado, A Jorio, et al. Origin of the 2450 cm^{-1} Raman bands in HOPG, single-wall and double-wall carbon nanotubes. Carbon 43 (2005) 1049-1054.

[32] P Tan, Y Deng, Q Zhao. Temperature-dependent Raman spectra and anomalous Raman phenomenon of highly oriented pyrolytic graphite. Physical Review B 58 (1998) 5435-5439.

- Second-order Raman spectroscopy can be used to characterise chars.
- A new deconvolution method has been established to characterize char structure.
- The char-H_2O and char-CO_2 gasification reactions follow different mechanisms.

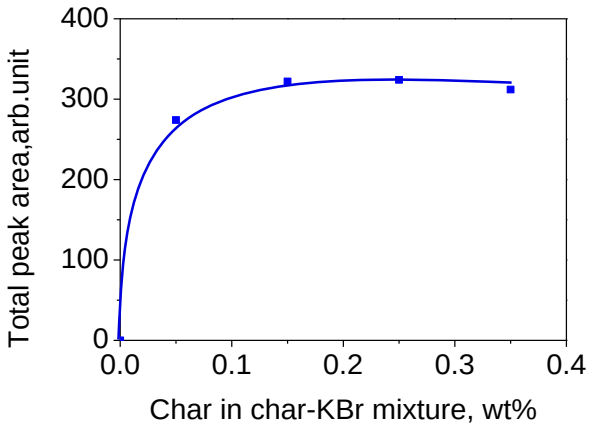

Fig. 1. Effects of char concentration in char-KBr mixture on the total second-order Raman area (2000-3300 cm^{-1}). Char was prepared from the gasification of the Collie sub-bituminous coal in 15% H_2O balanced with Ar at 900 ˚C.

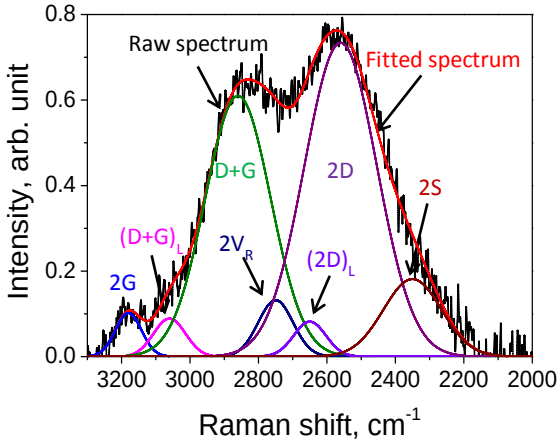

Fig. 2. Spectral deconvolution of a Raman spectrum (second-order region) of the char from the gasification of the Collie sub-bituminous coal in 15% H_2O balanced with Ar at 900 ˚C.

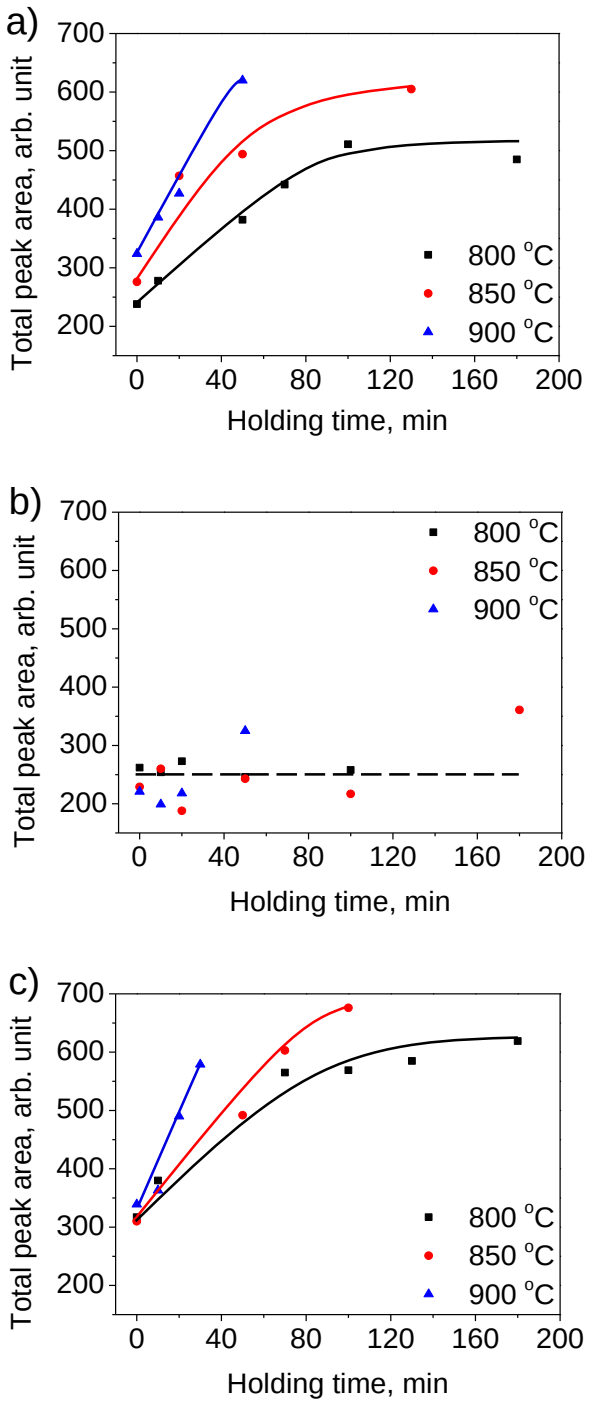

Fig. 3. Total second-order Raman area as a function of holding time for the chars from the gasification of Collie sub-bituminous coal at 800, 850 and 900 ˚C in (a) 15% H_2O balanced with Ar; (b) pure CO_2; (c) 15% H_2O balanced with CO_2.

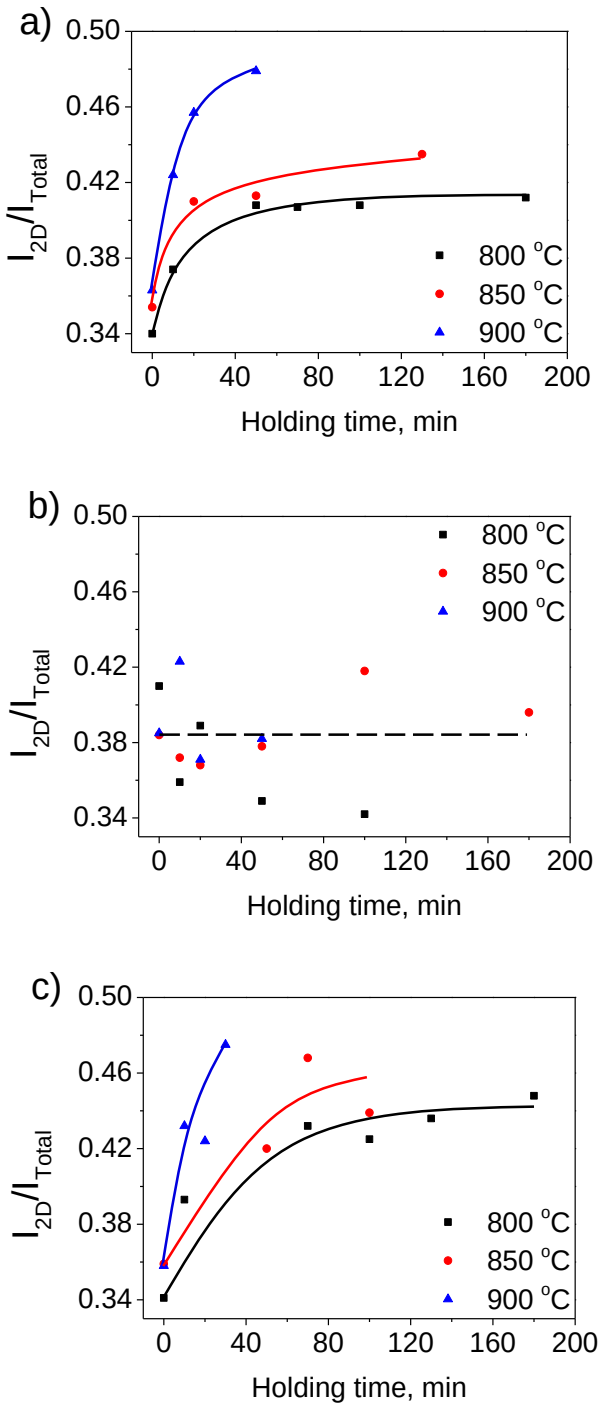

Fig. 4. Raman band area ratio 2D/Total as a function of holding time for the chars from the gasification of Collie sub-bituminous coal at 800, 850 and 900 ˚C in (a) 15% H_2O balanced with Ar; (b) pure CO_2; (c) 15% H_2O balanced with CO_2.

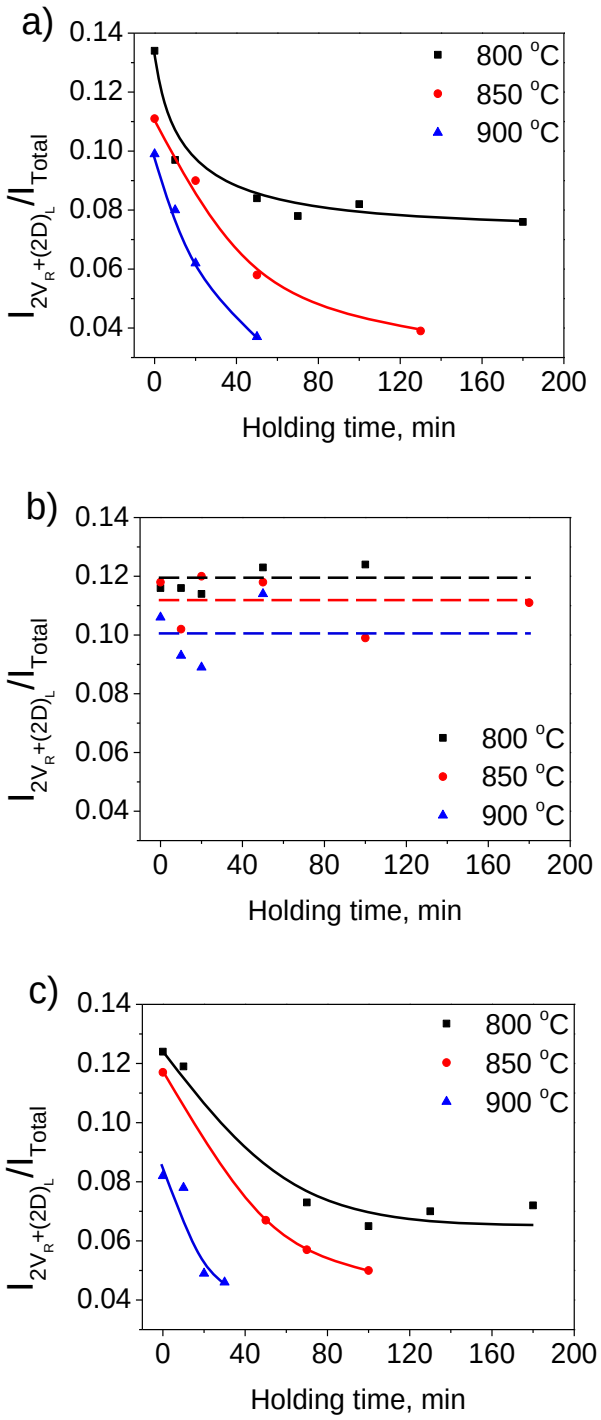

Fig. 5. Raman band area ratio $2V_R+(2D)_L$/Total as a function of holding time for the chars from the gasification of Collie sub-bituminous coal at 800, 850 and 900 ˚C in (a) 15% H_2O balanced with Ar; (b) pure CO_2; (c) 15% H_2O balanced with CO_2.

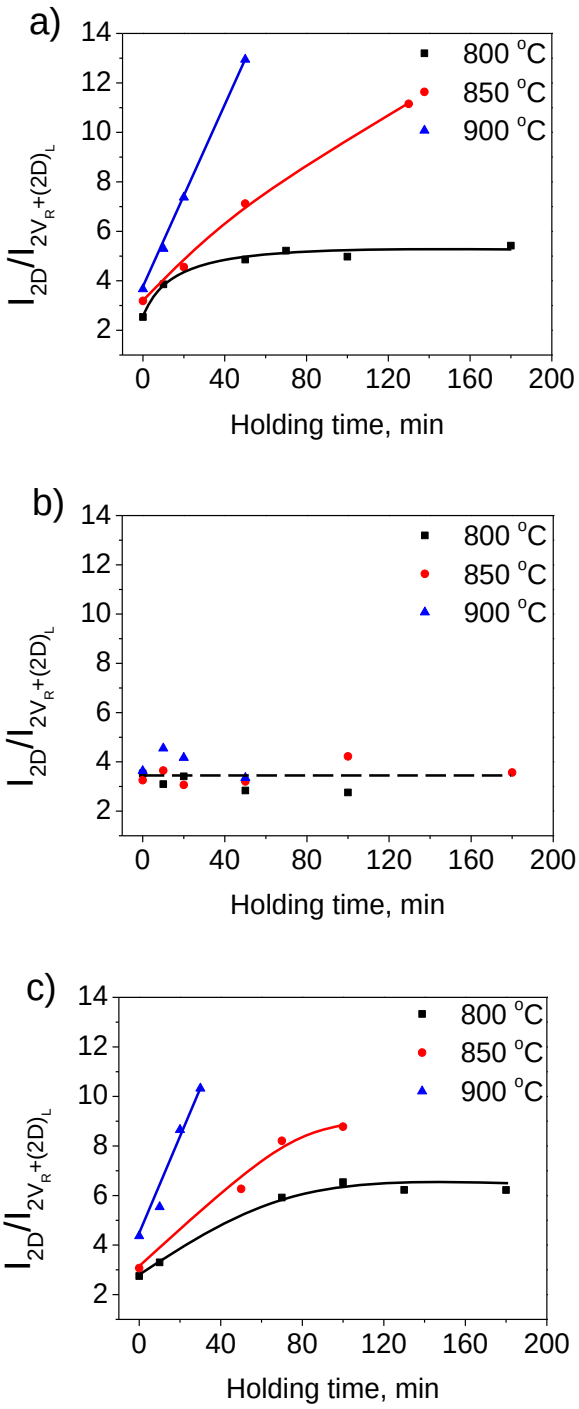

Fig. 6. Raman band area ratio $2D/2V_R+(2D)_L$ as a function of holding time for the chars from the gasification of Collie sub-bituminous coal at 800, 850 and 900 ˚C in (a) 15% H_2O balanced with Ar; (b) pure CO_2; (c) 15% H_2O balanced with CO_2.

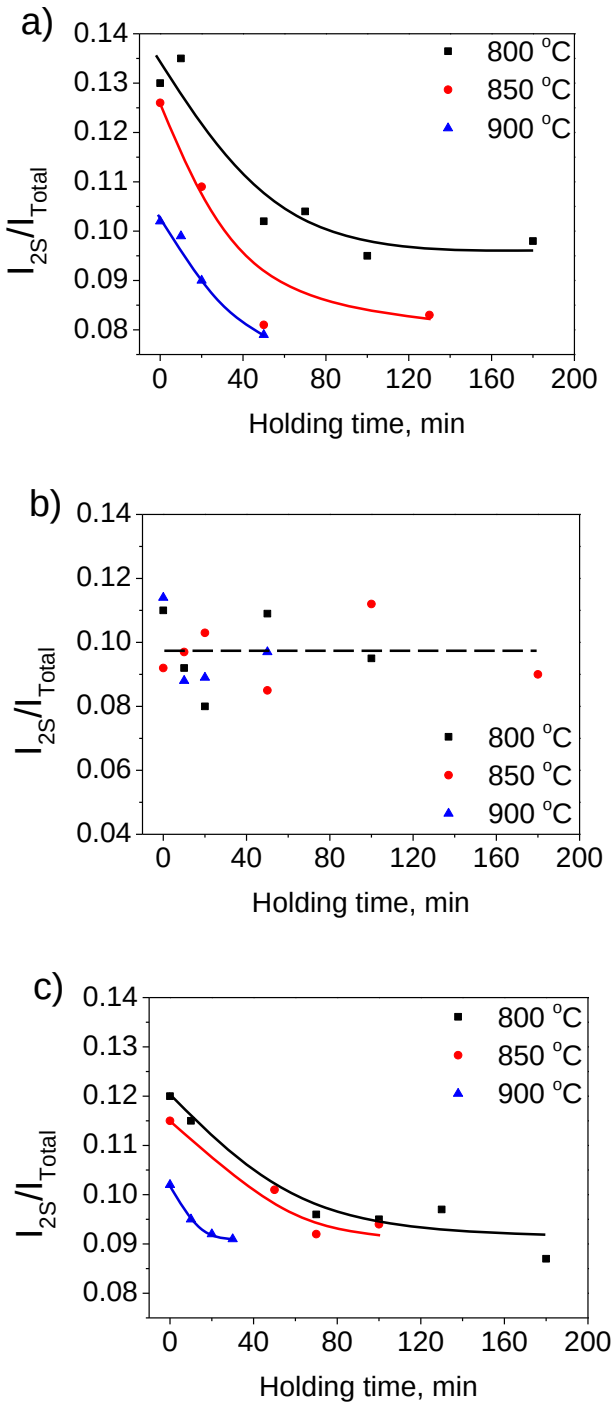

Fig. 7. Raman band area ratio 2S/Total as a function of holding time for the chars from the gasification of Collie sub-bituminous coal at 800, 850 and 900 ˚C in (a) 15% H_2O balanced with Ar; (b) pure CO_2; (c) 15% H_2O balanced with CO_2.

Table 1 Summary of peak/band assignment.

Band name	Band position, cm^{-1}	Description	Bond type	References
2G	3180	Overtone of G band; aromatic rings	sp^2	11,17, this work
$(D+G)_L$	3060	Aryl CH stretch vibration	sp^2	23
D+G	2860	Combination of D band and G band; aromatic rings	sp^2	11,17,24, this work
$2V_R$	2750	Overtone of the aryl CH_3 in-phase bend vibration; amorphous carbon structures	sp^2; sp^3	23
$(2D)_L$	2650	Small aromatic rings system; amorphous carbon structures	sp^2; sp^3	This work
2D	2560	Overtone of D band; C-C between aromatic rings; large aromatic rings system	sp^2	11,17,24, this work
2S	2350	Overtone of S band; $C_{aromatic}$-C_{alkyl}; C-C on hydroaromatic rings;	sp^2; sp^3	11,17, this work

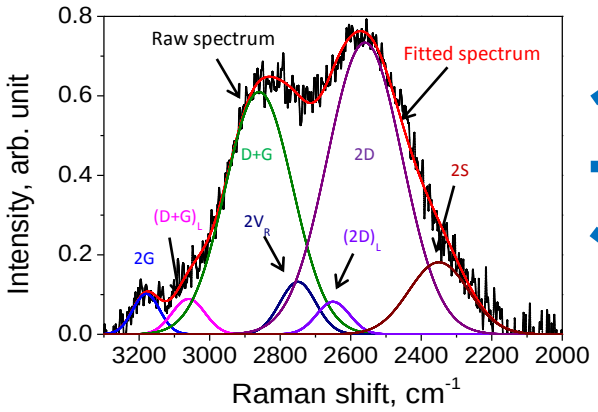

I_{Total}: The presence of O-containing structures.

$I_{2D}/I_{2VR+(2D)L}$: The transition of small to large aromatic ring systems.

I_{2S}/I_{Total}: The presence of alkyl-aryl C-C structures and other crossing-linking structures.